 DOI: 10.35382/TVUJS.14.8.2024.81

BUILDING A MODEL FOR TRACTION CONTROL USING AN ABS BRAKE ACTUATOR

Phan Tan Tai[1], Nguyen Khac Bang[2*]

Abstract – *In the anti-lock braking system, the brake actuator plays an indispensable role, regulating brake fluid to the brake cylinders on the wheels to perform the braking process following the system's requirements. Regulating brake fluid is a crucial and complex job that affects the effectiveness of the braking process as well as the traction control system of the brake actuator on the vehicle. In this article, the solution to control the brake actuator is proposed based on the control mode of the valves inside it, ensuring that the braking process on the wheels is consistent with their rolling state on the road surface, thereby controlling traction on the active wheels. To achieve this goal, the movement speed of the valves in the actuator and the brake fluid pressure at the wheel cylinders must be controlled by a special control algorithm. In addition, several model parameter variables are also considered. Simulation results are shown to demonstrate the effectiveness of the proposed control law.*

Keywords: ABS brake actuator, brake actuator control, brake fluid regulation, traction control.

I. INTRODUCTION

The anti-lock braking system (ABS) is recognized as an important contribution to road safety as it is designed to keep a vehicle moveable and stable during times of emergency braking by preventing wheel lock. The wheel will slip and lock when braking suddenly or when braking on a slippery road surface. This often causes a long stopping distance and sometimes the vehicle will lose steering stability [1, 2]. The goal of the ABS brake control system is to maintain wheel slippage for maximum friction and maintain steering stability throughout the car's movement. The system brings the car to a stop bringing the shortest possible distance while maintaining the car's steering direction. To achieve this ideal goal, the controller must control and adjust the wheel speed to suit the current conditions of the road on which the car is moving. In recent times, many ABS technologies have also been applied in traction control systems (TCS) and vehicle dynamic stability control [3]. The controller has been designed based on torque input to the driving wheels [4]. The output torque of the engine is controlled to achieve the control target of TCS through throttle control or the driver's accelerator pedal pressing state [5]. Another method that presented in many published research projects is to use braking torque on the active wheels to control the transmission of traction force on the active wheels through the ABS brake actuator [6–9] to control the wheel slip rate during acceleration on slippery roads or to transmit traction torque to the active wheels with high efficiency [10, 11].

To increase braking efficiency in the ABS braking system as well as in the traction control system, the movement speed of the valves in the actuator and the brake fluid pressure on the wheel cylinders must be controlled according to an algorithm specialized controls. Furthermore, model parameter variables are also considered and calculated properly. This study proposes a solution to control the brake actuator based on the control mode of the hydraulic valves inside it. To ensure that the braking process at the wheels is consistent with the wheel rolling state on the road surface, the models in the brake actuator are built accurately on the model parameters

[1,2]Tra Vinh University, Vietnam
*Corresponding author: nkbang@tvu.edu.vn
Received date: 02nd July 2024; Revised date: 17th July 2024; Accepted date: 22nd July 2024

determined from the beginning. The controller is designed and surveyed to evaluate the process of controlling traction on the active wheels.

II. ABS BRAKE ACTUATOR MODEL

The ABS system usually consists of three basic parts: the electronic control unit (ECU), the hydraulic control unit (HCU), and the wheel speed sensors. Figure 1 shows the typical structure of a part of the ABS hydraulic brake system, the system arranges the brake mechanism on the front and rear axle with disc brakes. During braking, the ECU controls the hydraulic pump to supply brake fluid pressure to the actuator pressure valves and deliver it to the wheel cylinders to perform the braking process according to the ECU's control program. The hydraulic brake actuator includes the following models: hydraulic pump model, accumulator model and hydraulic valve model.

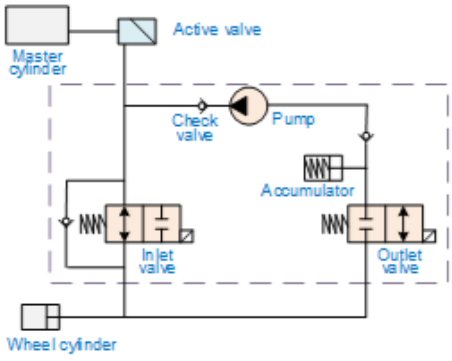

Fig. 1: Hydraulic circuit diagram for a wheel in an ABS brake actuator

A. Hydraulic pump model

In an hydraulic pump, the volume of the pressure chamber is determined according to Equation (1), in which: A is the cross-sectional area of the pump piston; e is the eccentricity of the pump cam; φ_0 is the initial angle of the pump cam; t is time.

$$V = A.e.\sin(\varphi_0 + \omega t) \qquad (1)$$

The flow and pressure of liquid through the pump are determined according to Equations (2) and (3). Here: p_{out} is the pressure in the pressure chamber; P_{in} is the suction chamber pressure; f is area ratio between pressure chamber and suction chamber.

$$Q_s = \dot{V} = A.e.\omega.\cos(\varphi_0 + \omega.t) \qquad (2)$$

$$p_s = p_{out} - f.p_{in} \qquad (3)$$

And the torque that the hydraulic pump resists back to the engine is calculated according to formula (4).

$$M_c = Q_s.p_s \qquad (4)$$

B. Accumulator model

The relationship between the length of the liquid chamber and the volume of the accumulator is as shown in Equations 5 and 6. In which: l_a is the length of the accumulator; x_o is the initial length of the energy storage cavity; x_1 is the displacement of the piston; d is the piston diameter.

$$l_a = x_0.x_1 \qquad (5)$$

$$V_a = l_a.\pi.d^2/4 \qquad (6)$$

The fluid flow entering the accumulator is determined by Equation 7. In which: v_a is the moving speed of the piston; ρ is the fluid density at pressure p_a; p_a is the pressure in the accumulator.

$$q_a = v_a.\frac{\pi}{4}d^2.\frac{\rho(p_a)}{\rho(0)} \qquad (7)$$

The dynamic equation of the piston is determined by Equations 8 and 9, in which: k is equivalent stiffness of the brake mechanism; m_p is the piston mass.

$$F_a = l_a.k - \frac{\pi}{4}d^2.p_a \qquad (8)$$

$$F_a = m_p v_a = m_p x_1 \qquad (9)$$

C. Hydraulic valve model

The commonly used oil inlet and outlet valves are solenoid valves, which act as high-speed magnetic switches. The basic structure of the solenoid valve is shown in Figure 2.

The current and moving speed of the valve are determined according to Equations (10), (11), and (12). In which: x, v are the displacement and speed of the valve needle; m is the volume of the valve needle; F_m, F_f are the electromagnetic force and resistance force; k is the elasticity of the valve spring; F_p is the fluid force component; b damping speed; G_o is the initial load of the spring.

$$\frac{di}{dt} = \frac{\left[U - R.i - i.v.\frac{\partial L(x,i)}{\partial i}\right]}{L(x,i) + i.\frac{\partial L(x,i)}{\partial i}} \quad (10)$$

$$\frac{dv}{dt} = \frac{1}{m}[F_m(x,i) - k(x + G_0) - F_p(x) - bv^3 - F_f] \quad (11)$$

$$\frac{dx}{dt} = -\frac{1}{\tau}x + \frac{k}{\tau}U \quad (12)$$

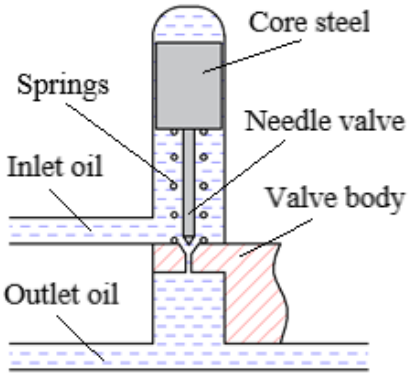

Fig. 2: Structure of solenoid valve

The oil flow through the valve when the valve is open is determined according to Equation (13), in which: C_d is the oil resistance coefficient, ρ is the oil density, A_f is the valve hole cross-section when the valve is open; p_s, p_c are the inlet and outlet oil pressure of the valve.

$$Q_c = C_d.A_f\sqrt{\frac{2}{\rho}(p_s - p_c)} \quad (13)$$

Assuming that the hole cross-section and opening of the inlet and outlet valves are the same and ignoring the resistance on the pipeline, the cross-sectional area of the valve hole when open is determined according to Equation (14), in which: d_0 is the diameter of the valve hole; X is the displacement stroke of the valve $(X \in t)$; α is the tilt angle of the valve.

$$A_f = \pi\frac{d_o^2}{4} - \pi.x.cos\alpha.(d_o + x.sin\alpha.cos\alpha) \quad (14)$$

If the pressure leaving the intake valve and the pressure reaching the wheel cylinder are considered to be the same, the pressure dynamic equation is determined by Equation (15). In which: β is the molecular mass of the brake oil, v_0 is the volume of the wheel cylinder.

$$\dot{p_c} = \frac{\beta}{v_0 + x.A_f}(Q_c - \dot{x}.A_f) \quad (15)$$

III. BUILDING AN ALGORITHM TO CONTROL THE ABS BRAKE ACTUATOR

The controller will control the active valve to close the oil line to the master cylinder, and activate the hydraulic pump to operate, providing hydraulic pressure to the wheel cylinder by controlling the hydraulic valves in three levels: pressure increase, pressure hold or pressure decrease during braking to ensure that the wheel does not slip on the road surface.

Assuming the inlet valve is opened, and the outlet valve is closed, the brake oil pressure to the wheel cylinder increases, and the oil pressure from the pump through the supply valve hole to the wheel cylinder according to Equation (15). Then the dynamic equation at the wheel is determined according to Equations (16) to (18). In which: M_i is the moment of inertia, ω is the angular speed of the wheel, M_p is the braking moment, k_b is the torque increase coefficient, p_c is the hydraulic pressure in the wheel cylinder, M_t is the traction moment of the wheel vehicle, F_t is the longitudinal force of the wheel, r_b is the

wheel radius.

$$M_i.\dot{\omega} = M_t - M_p \quad (16)$$

$$M_t = F_t.r_b \quad (17)$$

$$M_p = k_b.p_c \quad (18)$$

In this study, the Matlab Simulink software was used with PID control algorithm as shown in Figure 3 to control the oil flow in the wheel cylinder through controlling the opening and closing time of the inlet and outlet oil valves at the brake actuator. The output signal $u(t)$ applies voltage to the valve to maintain the open or closed state. This control algorithm is shown in Equation (19). Based on the value of the wheel speed deviation signal e(t), the ECU compares the actual fluid flow and the calculated oil flow to create a brake control signal e(t) sent to the ABS actuator, applying the braking torque to the brake mechanism at the wheel.

$$u(t) = K_p e(t) + K_i \int_0^t e(t)\,dt + K_d \frac{de(t)}{dt} \quad (19)$$

The PID controller is determined by the values K_p = 500, K_i = 10 and K_d = 0.1 through the selection process in Simulink to control the response according to the system requirements.

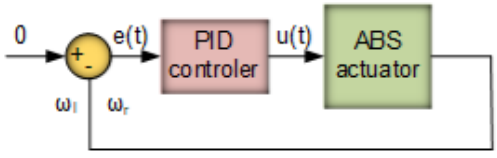

Fig. 3: PID controller diagram

IV. RESULTS AND DISCUSSION

When the vehicle runs straight on a road with varying grip on both sides of the driving wheel, the right wheel has good grip (MD-C), the left wheel has variable grip (completely slippery road surface - MD-A, light slippery road surface - MD-B, and good grip road surface - MD-C). The study surveyed model parameters such as traction power, car speed, slip coefficient, angular velocity on both sides of the wheel, traction force, and traction moment on the left and right wheels to evaluate the traction performance of the car by considering the traction force distribution on both sides of the driving wheel. The system parameters have the following values: supply hydraulic pressure $p_s = 60e^5$ Pa; the piston mass m_p = $150e^{-3}$ kg; equivalent stiffness of the brake mechanism $k = 4,654.57$ Nms/rad; solenoid valve opening voltage $U = 12$ VDC; the oil resistance coefficient $C_d = 85$ Ns/m; the oil density $\rho = 800$ kg/m^3; intake valve hole cross-section $A_f = 0.1385e^{-3}$ m^2.

A. In case the left wheel rolls on a slippery road surface (MD-A)

Engine power increased rapidly in the first and remained stable at N_e = 9,000 W throughout the survey period (Figure 4). The traction power on the left wheel is close to zero, at this time the engine power transmitted to the right wheel increases significantly, reaching the value N_t = 4,071 W and continuing to increase slightly during the survey period, at the end of the period survey time N_t = 4,315 W.

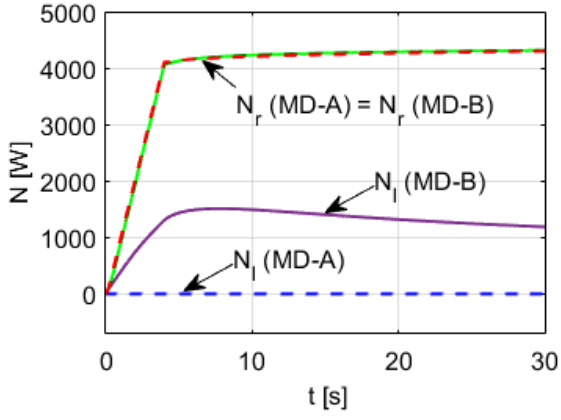

Fig. 4: Survey of traction capacity with PID controller at MD-A

The increased traction power of N_r with the above value helps the vehicle quickly overcome

slippery areas, causing the engine power transmitted to the wheels to not be wasted much, which leads to more efficient use of the engine's power, significantly increased compared to the case of not using this PID controller ($\eta_t = 47.94\%$). If this controller is not used, the car will not be able to move on surface MD-A, and engine power is wasted due to the left driving wheel over slipping [1–3]. The response ability of this PID controller is very good, after only 0.025s of impact, thereby showing that the designed controller meets control requirements.

The angular speeds on the right and left wheels increased gradually, were stable and equal, and at the end of the survey time the value $\omega_i = \omega_r = 29.05$ rad/s (Figure 5). When there is no controller, the right wheel speed is zero, making the vehicle unable to move, but when controlled, ω_r increases and is equal to ω_i, causing the car to move quickly through the slippery road surface slip. When using a PID controller, although ω_i is smaller than without a controller, the ω_i curve behavior with control is smoother and more stable than without control. This shows that when using a PID controller, the engine runs more stably (ω_e increases steadily), leading to stable vehicle movement.

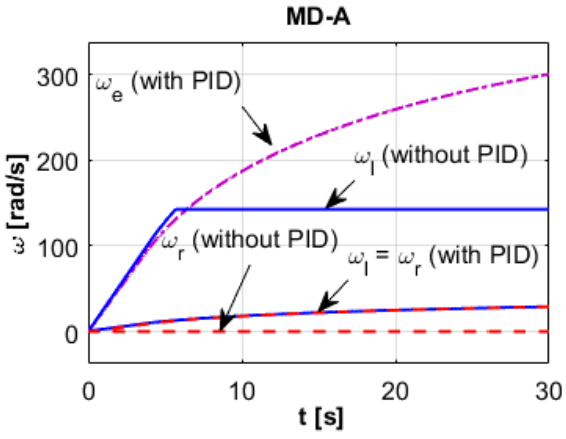

Fig. 5: Survey of wheels angular speed with PID controller at MD-A

When not in control, the difference in angular speed on both sides of the wheel is quite hight, because the slip coefficient on both sides of the wheel is much different: the left wheel rolls on the road surface of MD-A, and the right wheel rolls on the surface MD-C at the Figure 6a. On the contrary, when there is control, the slip coefficient of the left wheel (λ_1) is quickly reduced to the allowable threshold value (Figure 6b), causing the left wheel's angular speed to decrease and the right wheel's angular speed to increase. The vehicle must increase until the angular speeds of both sides of the driving wheels are equal (Figure 5). The left wheel slip coefficient increases to a maximum value of $\lambda_1 = 1$ at 0.5s, then rapidly decreases to the allowable slippage value $\lambda_1 = 30\%$ at 1.5s, causing the speed to decrease. The left wheel angle decreases rapidly and balances the speed of the right wheel.

The above slip coefficient value ensures that the two wheels actively rotate in a state where the road surface has slippage within the allowable threshold (below 30%). Therefore, the angular speeds of the two active wheels are stable and have equal values.

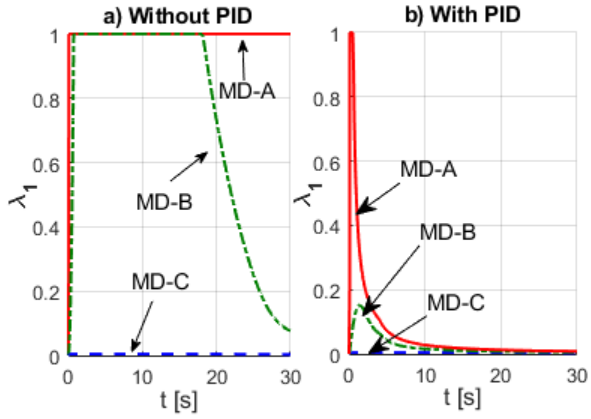

Fig. 6: Left wheel slip coefficient with PID controller

The traction force on both sides of the wheel changes significantly when using a PID controller compared to when not using one. With the PID controller, the traction on the right wheel (F_i) is much greater than on the left wheel (F_i) (Figure 7), making it easier for the car to navigate

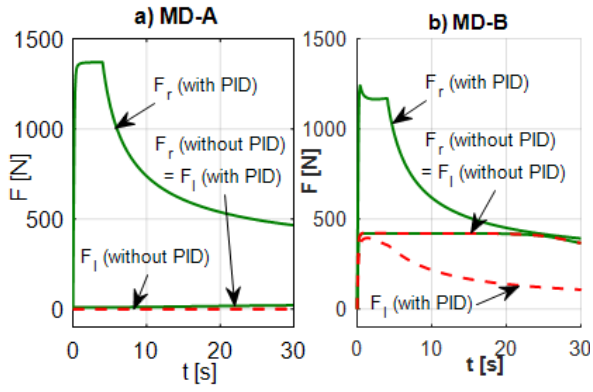

Fig. 7: Traction force on the active wheel with PID control

slippery areas. The traction on the left wheel (F_i) is close to zero, as the braking moment acting on the left wheel increases the moment of inertia on the right wheel, leading to increased traction. The traction force on the right wheel increases rapidly in the first 4.025s to a value of $F_r = 1,371$ N, then gradually decreases to $F_r = 466$ N by the end of the survey period. The decrease in traction force during this time is due to a steady increase in the right wheel's angular speed, leading to a decrease in the moment of inertia and a subsequent decrease in the traction force. Therefore, the more braking torque acting on the left wheel, the more traction on the right wheel increases, depending on the stable speed of the wheel. The more stable the angular speed of the wheel, the more the moment of inertia decreases, causing the traction force at the wheel to decrease.

B. In case the left wheel rolls on a light slippery road surface (MD-B)

The traction capacity of the two active wheels is more stable than in the case of not using a PID controller. The right wheel traction power has the same behavior as the MD-A case but the value increases slightly at 4.025s (N_r = 4,112 W) and reaches the value N_r = 4,297 W at the end survey time (Figure 8). When using PID control, traction power N_r increases quickly and is stable at 4.025s, while without using the controller N_rs increases slowly and is stable at the end survey period. This shows that the PID controller responds promptly to the distribution of traction torque at the active wheels.

Traction power at the left wheel increases more slowly than in the N_r and reaches value N_i = 1,506 W at 7s, then decreased slightly to N_i = 186 W at the end of the survey. The N_i power value is much smaller and more stable than the case without using a PID controller, this shows that thanks to the braking torque acting on the left wheel, the slippage of the left wheel is reduced fast and within allowable limits (Figure 6).

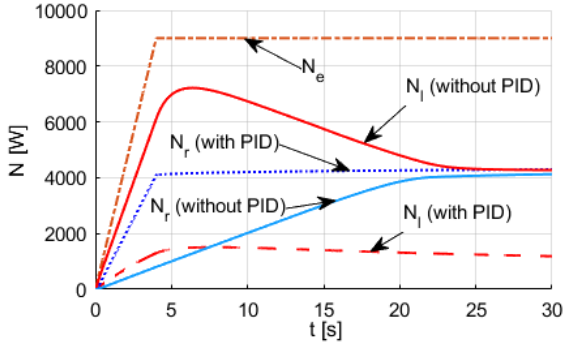

Fig. 8: Survey of traction capacity with PID controller at MD-B

When using the PID controller in case the left wheel rolls on the road surface of MD-B, the engine's power utilization efficiency $\eta_t = 60.92\%$, this value is reduced compared to the case of not using the PID controller. The reason is that part of the power is consumed by braking on the left wheel. The response-ability of the PID controller, in this case, is the same as the case where the left wheel rolls on the road surface MD-A.

The N_r power increase is hightly due to the increased angular speed at the right wheel. The angular speeds on the right and left wheels gradually increase, are stable, and have equal values, at the end of the survey time the value $\omega_i = \omega_r = 34.26$ rad/s (Figure 9). The angular speed ω_i when using the PID controller is smaller than without the controller, but the curve

behavior ω_i with control is smoother and more stable than the angular speed of the left wheel without control. This shows that when using a PID controller, the engine runs more stably (ω_e increases steadily), leading to the car's movement being stable. In addition, the angular speed on both sides of the active wheel when using the PID controller is likely to be stable and highly responsive compared to not using the controller (the angular speed on both sides of the wheel is stable at the right time the end of the survey process). If without this PID, the engine power is wasted due to wheel slippage [1–3].

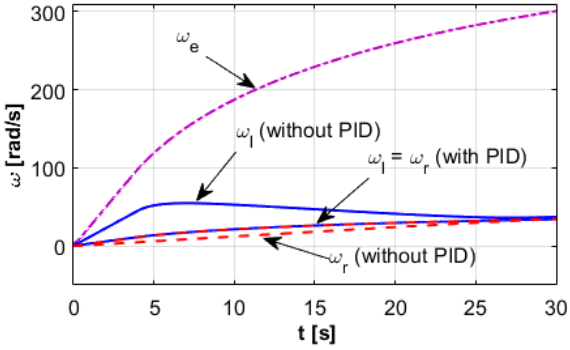

Fig. 9: Survey of wheel angular speed with PID controller at MD-B

In case the left wheel rolls on MD-B, the traction force on both sides of the wheel has a large change in value compared to the case where the PID controller is not used. When not using the PID controller, the traction force on both sides of the active wheel is always equal. When in control, the traction on the right wheel (F_r) is greater than the traction on the left wheel (F_i), causing the car to quickly overcome slippery areas. The value of traction on the left wheel is reduced compared to the uncontrolled case (Figure 7), because at this time the braking moment acting on the left wheel causes the moment of inertia on the right wheel to increase, leading to increased force drag F_r higher than F_i. The left wheel traction value increased the most at F_i = 395 N at 1.34 s, then gradually decreased until the end of the survey time, reaching F_i = 108 N. The right wheel traction force increases rapidly to the value F_r = 1,241 N at the first 0.34s, then decreases slightly to the value F_r = 1,170 N at the time 4.025 s, then continues gradually decreased until the end of the survey period reaching F_r = 392.7 N. The decreased traction during this time is due to the steady increase in angular speed on both sides of the wheel, leading to a decrease in the moment of inertia, causing the traction forces (F_i) and F_r to decrease. Although the F_r traction force value is smaller than the case where the left wheel rolls on road surface MD-A, in return the traction force on the left wheel increases, leading to the angular speed of both sides of the wheel in both cases MD-B and MD-A having the same values (Figure 5 and Figure 9). Therefore, the lower the value of the braking torque acting on the left wheel, the lower the traction force on the right wheel. However, this also depends on the stability of the angular speed of the two sides of the active wheel. The more stable the angular speed of the two sides of the wheel is the more, the moment of inertia decreases, which is causing the traction force at the wheel to decrease.

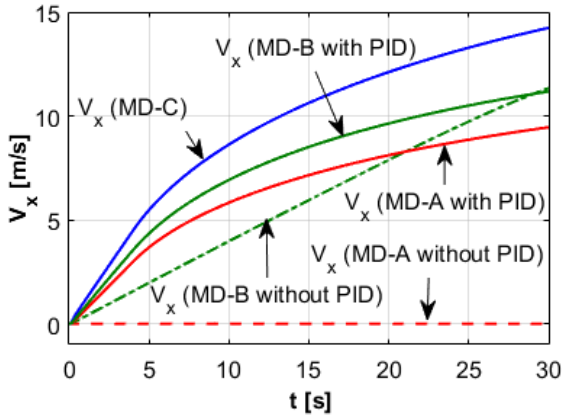

Fig. 10: Vehicle speed when using the PID controller

When the slip coefficient changes, the wheels rotate at different angular speeds, causing the car's speed to change. When using the PID controller, the car's speed increases as the left wheel's grip increases (Figure 10), and the car's

speed increases along a curve: when the left wheel rolls on the road surface MD-A V_x = 9.46 m/s, the left wheel rolls on the road surface MD-B V_x = 11.18 m/s. In case the controller is not used, the vehicle speed depends on the grip of the left wheel with the road surface: corresponding to the case where the left wheel rolls on the road surface MD-A V_x = 0, the car cannot moving; the left wheel rolls on the road surface of MD-B, the car speed increases linearly and reaches a speed at the end of the survey time with the value V_x = 11.34 m/s. Survey results show that when using a controller, the car's speed increases more stably, because V_x increases in a uniform curve, and the angular speeds of both sides of the active wheel being controlled have equal values. If a controller is not used, V_x increases linearly, due to the different angular speeds of both sides of the wheel, the moment of inertia generated at the rapidly rotating wheel is large, leading to unstable vehicle movement. At the same time, when one side of the wheel slips completely, the vehicle cannot move, causing a loss of engine power.

When using a PID controller to control the traction power of a car, this controller compares the difference in angular speed (e) of the two sides of the active wheel, if the value e exceeds the allowable threshold ($|\varepsilon|$), the PID controller will output a brake torque signal with an appropriate value to brake the slipping wheel (M_p). The higher the value of the slip coefficient between the wheel and the road surface, the greater the braking moment acting on the wheel (Figure 11). This causes the angular speed of the sliding wheel to decrease, resulting in the error value gradually approaching zero, helping the angular speeds of the two sides of the active wheel get closer to each other. Therefore, the differential distributes traction power to the wheels with great value, helping the car move stably on the road, reducing engine power consumption, and improving the car's traction performance. This approach is novel compared to the in-wheel-motor control method to reduce wheel slipping [11, 12], as well as control the engine torque through throttle angle control [4], optimal slip ratio algorithm or PID fuzzy logic method [6, 7].

The survey results of errors in the angular speed between the two sides of the wheel have a very low value, $e = 0.88$ rad/s, the angular speed difference value between the two sides of the active wheel decreases as the grip between the tires and the road surface increases (Figure 12). Thereby, using the PID controller to apply braking torque to the slipping wheel helps the differential distribute traction power to the two wheels by the grip condition between the tire and the road surface, to improve engine power efficiency. When using braking torque to act on the slipping wheel, part of the power is consumed by braking, causing the car's traction power efficiency to decrease ($\eta_t = 47.94\%$). However, the car still moves stably through slippery road surfaces, especially when one wheel completely slips.

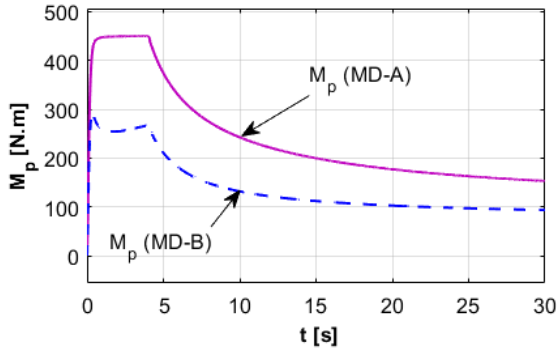

Fig. 11: Braking torque acting on the left wheel when controlled by PID

V. CONCLUSION

The proposed brake actuator control solution to control traction force on the active wheels when they spin on the road surface, which improves the engine's capacity efficiency. This PID control algorithm is built based on models in the brake actuator and the operating status of the active wheels. The survey results compared with the case of not using a controller have the evaluation criteria reached high values. This shows that the

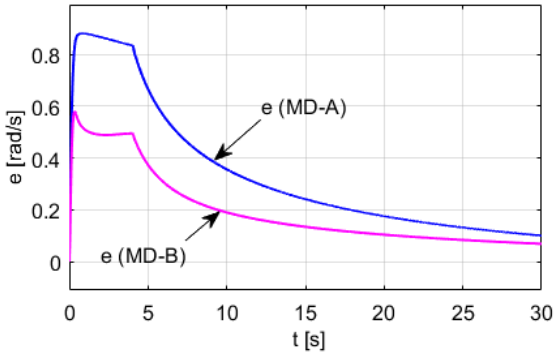

Fig. 12: Error of the angular speed on both sides of the wheel with PID controller

method of controlling traction through controlling the brake actuator achieves high efficiency. However, when the vehicle starts on a slippery road with a very low grip on both sides of the wheel, using this PID controller may not be possible, because the engine's ability to receive power on both sides of the tire at this time does not meet the requirements. Therefore, the engine power should be reduced to match the grip ability of both sides of the active wheels. This will be specifically researched by the team in the next project.

REFERENCES

[1] Mauer GF. A fuzzy logic controller for an ABS braking system. *IEEE Transactions on Fuzzy Systems*. 1995;3(4): 381–388. https://doi.org/10.1109/91.481947.

[2] Lennon WK, Passino KM. Intelligent control for brake systems. *IEEE Transactions on Control Systems Technology*. 1999;7(2): 188–202. https://doi.org/10.1109/87.748145.

[3] Aly A, Zeidan E, Hamed A, Salem F. An antilock-braking systems (ABS) control: A technical review. *Intelligent Control and Automation*. 2011;2(3): 186–195. https://doi.org/10.4236/ica.2011.23023.

[4] Kabganian M, Kazemi R. A new strategy for traction control in turning via engine modeling. *IEEE Transactions on Vehiclar Technology*. 2001;50(6): 540–1548. https://doi.org/10.1109/25.966584.

[5] Tan HS, Chin YK. Vehicle traction control: Variable structure control approach. *Journal of Dynamic Systems, Measurement, and Control*. 1999;113(2): 223–230. https://doi.org/10.1115/1.2896369.

[6] Liu G, Jin L. A study of coordinated vehicle traction control system based on optimal slip ratio algorithm. *Mathematical Problems in Engineering*. 2016;2016(1): 1–10. http://dx.doi.org/10.1155/2016/3413624.

[7] Li HZ, Li L, He L, Kang MX, Song J, Yu LY, et al. PID plus fuzzy logic method for torque control in a traction control system. *International Journal of Automotive Technology*. 2012;13(3): 441–450. https://doi.org/10.1007/s12239-012-0041-4.

[8] Tai PT, Nhu TV, Dung TQ. Using the brake torque to redistribute the engine power transmitting to the left and right drive wheels. In: Long BT, Kim YH, Ishizaki K, Toan ND, Parinov IA, Vu NP (eds.). *Proceedings of the 2nd Annual International Conference on Material, Machines and Methods for Sustainable Development (MMMS2020)*. Cham: Springer; 2021. p.502–507. https://doi.org/10.1007/978-3-030-69610-8_69.

[9] Park Y, Kwak B. Slip controller design for a traction control system. *International Journal of Automotive Technology*. 2000;1(1): 48–55.

[10] Saha S, Ikkurti HP, Saha S. A robust slip based traction control of an electric vehicle under different road conditions. In: *Michael Faraday IET International Summit: MFIIS-2015*. 12^{th}–13^{th} September 2015; Kolkata, India. IEEE; 2015. p.124–131. https://doi.org/10.1049/cp.2015.1618.

[11] Nam K, Hori Y, Lee C. Wheel slip control for improving traction-ability and energy efficiency of a personal electric vehicle. *Energies*. 2015;8(7): 6820–6840. https://doi.org/10.3390/en8076820.